



## Investigation on polymer anode design for flexible polymer solar cells

Yinhua Zhou, Fengling Zhang, Kristofer Tvingstedt, Sophie Barrau, Fenghong Li, Wenjing Tian, and Olle Inganäs

Citation: [Applied Physics Letters](#) **92**, 233308 (2008); doi: 10.1063/1.2945796

View online: <http://dx.doi.org/10.1063/1.2945796>

View Table of Contents: <http://scitation.aip.org/content/aip/journal/apl/92/23?ver=pdfcov>

Published by the [AIP Publishing](#)

---

### Articles you may be interested in

[Interface investigation of the alcohol-/water-soluble conjugated polymer PFN as cathode interfacial layer in organic solar cells](#)

J. Appl. Phys. **114**, 113709 (2013); 10.1063/1.4821223

[Enhancement of efficiency of a conducting polymer P3HT:CdSe/ZnS quantum dots hybrid solar cell by adding single walled carbon nanotube for transporting photogenerated electrons](#)

J. Renewable Sustainable Energy **5**, 033107 (2013); 10.1063/1.4807475

[Solution processed LiF anode modification for polymer solar cells](#)

Appl. Phys. Lett. **100**, 253303 (2012); 10.1063/1.4729932

[Large-area organic solar cells with metal subelectrode on indium tin oxide anode](#)

Appl. Phys. Lett. **96**, 173301 (2010); 10.1063/1.3419925

[Role of tungsten oxide in inverted polymer solar cells](#)

Appl. Phys. Lett. **94**, 043311 (2009); 10.1063/1.3076134

---

The image shows the cover of the journal Applied Physics Reviews. It features a blue and orange color scheme with a molecular structure in the background. The text 'AIP Applied Physics Reviews' is at the top left. The main title 'NEW Special Topic Sections' is in large white letters. Below it, 'NOW ONLINE' is in yellow, followed by 'Lithium Niobate Properties and Applications: Reviews of Emerging Trends' in white. The AIP logo and 'Applied Physics Reviews' are at the bottom right.

**NEW Special Topic Sections**

**NOW ONLINE**  
Lithium Niobate Properties and Applications:  
Reviews of Emerging Trends

**AIP** Applied Physics  
Reviews

# Investigation on polymer anode design for flexible polymer solar cells

Yinhua Zhou,<sup>1,2</sup> Fengling Zhang,<sup>1,a)</sup> Kristofer Tvingstedt,<sup>1</sup> Sophie Barrau,<sup>1</sup> Fenghong Li,<sup>1</sup> Wenjing Tian,<sup>2</sup> and Olle Inganäs<sup>1</sup>

<sup>1</sup>Department of Physics, Chemistry and Biology (IFM), Linköping University, SE-581 83 Linköping, Sweden

<sup>2</sup>State Key Lab for Supramolecular Structure and Materials, Jilin University, 130012 Changchun, People's Republic of China

(Received 18 April 2008; accepted 22 May 2008; published online 13 June 2008)

Bilayer polymer anode composed of poly(3,4-ethylene-dioxythiophene): polystyrenesulfonate (PEDOT:PSS) (PH500) and PEDOT:PSS (Baytron P VP Al 4083) was used to construct flexible polymer solar cells on plastic substrates polyethylene terephthalate (PET) with a device structure of PET/polymer anode/APFO-3:PCBM/LiF/Al. The power conversion efficiency (PCE) of the indium tin oxide (ITO)-free solar cells achieved 2.2% under illumination of AM1.5 (100 mW cm<sup>-2</sup>), which is 80% of the PCE of the reference cells with ITO on glass. The simplicity of preparing bilayer polymer anode and the comparable performance achieved in the flexible solar cells made the bilayer polymer anode an alternative to ITO for flexible solar cells produced by printing technology.  
© 2008 American Institute of Physics. [DOI: 10.1063/1.2945796]

Polymer solar cells have been the subject of extensive research in the past decade resulting in considerable progress in cell performance. Recently the power conversion efficiency (PCE)  $\sim 5.5\%$  was reached in single-junction polymer solar cells<sup>1,2</sup> and  $\sim 6.5\%$  in double-junction cells.<sup>3</sup> Polymer solar cells offer several inherent advantages over inorganics. The most important specialty is mechanical flexibility, which facilitates for coating onto flexible substrates, the prerequisite for roll to roll processing. Accordingly, researchers tried to fabricate devices on flexible substrates. Al-Ibrahim *et al.*<sup>4</sup> reported polymer solar cells on flexible indium tin oxide (ITO)-coated polyester foils with PCE  $\sim 3\%$ , which is comparable to the cells on ITO-coated glass substrate. However, the use of such flexible substrates presents technological challenges because plastics suffer from thermal shrinkage when ITO is deposited. In order to realize fully flexible polymer solar cells and replace ITO, researchers sought some anode materials to substitute the ITO.<sup>5-8</sup> Recently, a highly conductive poly(3,4-ethylene-dioxythiophene): polystyrenesulfonate (PEDOT:PSS) Baytron PH500 (hereafter referred to as PH500) was used as polymer anode to replace ITO in organic light-emitting diodes (OLEDs).<sup>9</sup> OLEDs with PH500 anode had comparable efficiencies and even surpassed, in some cases, the efficiencies achieved from ITO-based devices.<sup>9</sup> Very recently, Ahlswede *et al.*<sup>10</sup> reported efficient polymer solar cells using two different doped forms of PH500 on top of each other, as anode on glass substrates using high temperature annealing. Here, we demonstrate that 80% of the PCE of standard solar cells with ITO on glass was achieved in the flexible polymer solar cells on transparent plastic substrates polyethylene terephthalate (PET) by using bilayer polymer anode PH500/PEDOT [Baytron P VP Al 4083, electroluminescent (EL) grade] with low temperature processing, with a device structure of PET/PH500/PEDOT-EL/APFO-3<sup>6</sup>:PCBM/LiF/Al under illumination of AM1.5 (100 mW cm<sup>-2</sup>), which indicates the possibility to produce efficient flexible large-area polymer solar cells by roll to roll process where APFO-3

is an alternating polyfluorene copolymer poly[2,7-(9,9-dioctyl-fluorene)-alt-5,5-(4',7'-di-2thienyl-2',1'3'-benzothiadiazole)] and PCBM is [6,6]-phenyl-C61-butyric acid methyl ester.

The flexible PET substrate is from Hifi Industrial Film® (PMX739, 250  $\mu$ m, 88.7% light transmittance). The PH500 is from H. C. Starck. The 5% dimethylsulfoxide and zonyl surfactant were added into the PH500 to enhance the conductivity and wetting, respectively. The single layer anode of PH500 and bilayer anode PH500/PEDOT-EL were prepared on PET under the same conditions for transmission, sheet resistance measurements, and morphology imaging as used in the devices shown in Fig. 1(a), except for ultraviolet photoelectron spectroscopy (UPS) measurement, in that case, PH500 was deposited on glass substrate. The PH500 film was prepared by spin coating on cleaned PET or glass for 10 s at a speed of 800 rpm and then left to dry for  $\sim 5$  min under a gentle air flow to get a relatively thick film for lower sheet resistance. Then the films were heated at 72 °C (lower than the PET's glass transition temperature) for 3 h to remove the water. Its thickness is  $\sim 200$  nm. PEDOT-EL ( $\sim 50$  nm) as the second layer of polymer anode was spin coated (2500 rpm) on dried PH500 and heated for 1 h at 72 °C.

For comparison, devices with different anodes were fabricated under the same conditions by spin coating the active layers composed of APFO-3:PCBM<sup>6</sup> (1:3, weight ratio) from chloroform solution on glass/ITO/PEDOT-EL as reference cells (device 1) or PET/PH500 (device 2) or PET/

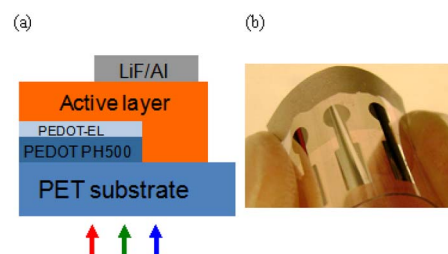


FIG. 1. (Color online) (a) The device structure and (b) a photograph of flexible solar cells.

a) Author to whom correspondence should be addressed. Electronic mail: fenzh@ifm.liu.se.

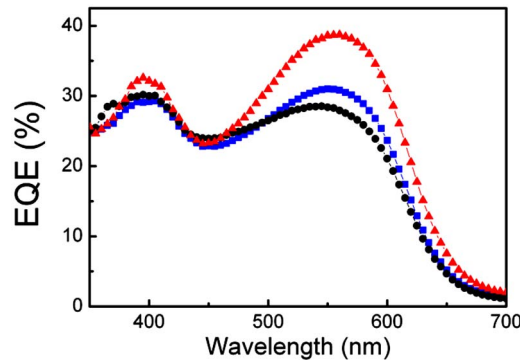


FIG. 2. (Color online) EQEs of three devices: device 1 (triangle), device 2 (square), and device 3 (circle).

PH500/PEDOT-EL (device 3). The thickness of the active layer was about 90 nm. The interfacial layer LiF (0.6 nm) and top electrode Al (60 nm) were deposited in vacuum. The effective area of the devices is 4–6 mm<sup>2</sup>. The device structure and a photograph of the flexible polymer solar cells were shown in Figs. 1(a) and 1(b).

The transmission spectra were recorded using a spectrophotometer (Lambda 950). The sheet resistances were measured by a four-point probe and the work functions were evaluated by UPS. The topography of the films was imaged by atomic force microscopy (AFM) with a Dimension 3100 system operating in tapping mode. Device fabrication and characterization were performed in an ambient environment as previously reported.<sup>8</sup>

To be used as an electrode in solar cells, conductivity, work function, and transmittance are important parameters to be considered. The sheet resistance of the PET/PH500 (~200 nm) was about 230 Ω/sq, which corresponded to the film conductivity of ~220 S cm<sup>-1</sup>. The work function of PH500 on glass evaluated by UPS was 5.0 eV. The transmittance of PET/PH500 was about 75% in most of the visible region while the glass/ITO/PEDOT-EL (50 nm) has the transmittance of 85%–90%.<sup>11</sup> The difference in transmittance originated from lower transmission of the PET substrate (88.7% light transmittance) than ITO/glass, and the absorbance of the thick PH500 layer.

First, devices 1 and 2 were fabricated and characterized. The external quantum efficiencies (EQEs) of two devices were depicted in Fig. 2. It was observed that the EQE of the device 2 was lower than that of device 1, probably due to the lower transmittance of PET and the PH500 layer. The shapes of EQEs were slightly different because the optical field distributions in the active layers were modulated by different substrates and anodes. The *J*-*V* characteristics of these two devices under illumination of 100 mW cm<sup>-2</sup> were recorded (Fig. 3) and summarized in Table I. The flexible device 2 exhibited a short-circuit current density (*J*<sub>sc</sub>) of 4.15 mA cm<sup>-2</sup>, which was ~12% lower than that of device 1 (4.70 mA cm<sup>-2</sup>). This reduction of *J*<sub>sc</sub> from device 1 to device 2 matches with the decrease in transmittance between glass/ITO/PEDOT-EL (85%–90%) and PET/PH500 (75%) (Ref. 11) and indicate that the transmittance play a major role to reduce *J*<sub>sc</sub>.

It was surprising that fill factor (FF) and open-circuit voltage (*V*<sub>oc</sub>) of device 2 were more than 10% lower than those of device 1. Device 1 presented a *V*<sub>oc</sub> of 1.02 V, a typical value of APFO-3 blended with PCBM for solar

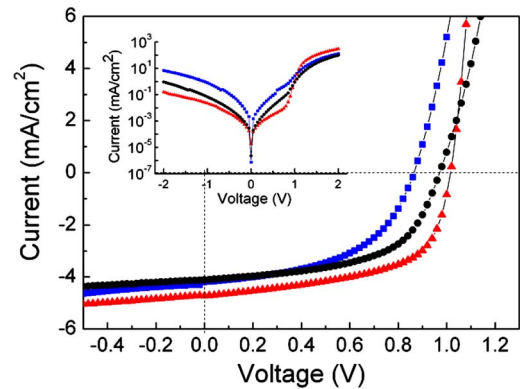


FIG. 3. (Color online) Current-voltage (*J*-*V*) characteristics of three devices under AM1.5 illumination (100 mW cm<sup>-2</sup>) and in dark (inset), device 1 (triangle), device 2 (square), and device 3 (circle).

cells,<sup>12</sup> but device 2 only reached a *V*<sub>oc</sub> of 0.86 V. It is well known that *V*<sub>oc</sub> is influenced mainly by the difference between the highest occupied molecular orbital level of donor and the lowest unoccupied molecular orbital level of acceptor<sup>13</sup> as well as the work function difference between two electrodes.<sup>14</sup> The active layers and cathodes of the two devices are exactly same. The work function of glass/ITO/PEDOT-EL (~50 nm) evaluated by UPS is similar to PH500 (5.0 eV); therefore, some other reasons must be responsible for the *V*<sub>oc</sub>'s reduction from 1.02 to 0.86 V. The inset of Fig. 3 showed the *J*-*V* characteristics of two devices in dark in semilog axis. Much higher dark current in reverse voltage and low forward voltage region (from 0 V to ~*V*<sub>oc</sub>) of device 2 than that of device 1 was observed. The shunt resistance (*R*<sub>sh</sub>) of device 2 calculated from *J*-*V* curve was 1.06 kΩ cm<sup>2</sup>, lower than that of the device 1 (1.75 kΩ cm<sup>2</sup>), which indicated that leak current decrease the *V*<sub>oc</sub>, possibly due to the high conductivity and rough surface of PH500. Similar phenomenon was also reported, the higher conductive PEDOT used as buffer layer made the *V*<sub>oc</sub> of the device reduce from 1.0 to 0.85 V.<sup>15</sup>

To confine the dark leak current and to enhance the *V*<sub>oc</sub> of device 2, a thin PEDOT-EL layer was added on the top of dried PH500. The bilayer polymer anode flexible devices were fabricated with a structure of PET/PH500/PEDOT-EL/APFO3:PCBM/LiF/Al (device 3). EQE and *J*-*V* of device 3 were presented together with other two types of devices in Figs. 2 and 3, respectively. The photovoltaic parameters of all three devices were summarized in Table I, which showed that PEDOT-EL not only enhance the *V*<sub>oc</sub> to 0.98 V, approaching to that of device 1 (1.02 V), but also the rectification ratio at ±2 V was increased by about one order of magnitude compared to device 2 due to reduced dark current (inset of Fig. 3) under reverse bias. The *R*<sub>sh</sub> was increased from 1.06 to 1.58 kΩ cm<sup>2</sup>, therefore, FF was improved from 0.51 to 0.56, approaching to that of device 1.

TABLE I. The performances of three devices under illumination of 100 mW cm<sup>-2</sup>.

Devices	<i>J</i> <sub>sc</sub> (mA cm <sup>-2</sup> )	<i>V</i> <sub>oc</sub> (V)	FF (%)	PCE (%)	<i>R</i> <sub>sh</sub> (KΩ cm <sup>2</sup> )
1	4.70	1.02	58	2.78	1.75
2	4.15	0.86	51	1.82	1.06
3	4.06	0.98	56	2.23	1.58



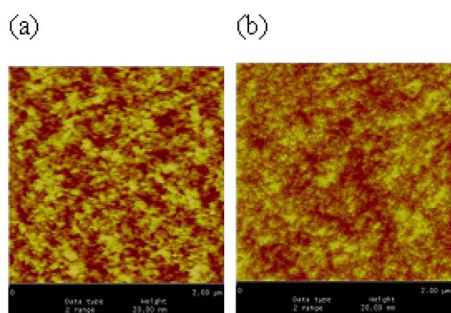


FIG. 4. (Color online) AFM images of the topography (a) PET/PH500 and (b) PET/PH500/PEDOT-EL. The scan size was  $2 \times 2 \mu\text{m}^2$  and Z range was 20 nm.

The  $J_{sc}$  and EQE were slightly lower than those of device 2 and the overall PCE of device 3 is 2.23%, which was 80% of device 1 (2.78%).

To investigate the functions of PEDOT-EL layer in device 3, the transmittance and topography of bilayer polymer anode were checked. The transmittance of bilayer anode was slightly lower than single layer PH500 anode,<sup>11</sup> which might be responsible for a little lower EQE and  $J_{sc}$  of device 3 than device 2. As we mentioned before, the work function of PH500 and PEDOT-EL were same. The two parameters that could be influenced by adding PEDOT-EL layer on the top of PH500 would be conductivity and morphology. The morphology of PET/PH500 and PET/PH500/PEDOT-EL were imaged by AFM (Figure 4), [4(b)] PET/PH500/PEDOT-EL presented a smoother surface than [4(a)] PET/PH500. The height scales of AFM images were 20 nm. Significantly smoothed the surface of PH500 by adding PEDOT-EL should be one reason for improved PCE of device 3 via  $V_{oc}$  and FF. In addition, PEDOT-EL is well known as a low conductive PEDOT, commonly used as a buffer layer in organic LED and solar cells. Similar function of PEDOT-EL was observed in device 3, that is, efficiently blocked the dark leaky current from highly conductive and rough PH500, and which resulted in an enhanced  $V_{oc}$ , FF, and PCE. To evaluate the performance of the flexible solar cells more convincingly, 15 cells for each type (totally 45 cells) were fabricated and characterized. All the photovoltaic data showed the same trend in statistical graphs<sup>11</sup> as that in Fig. 3 and Table I.

In conclusion, polymer solar cells on flexible substrate PET using single layer or bilayer polymer PEDOT:PSS as anodes were fabricated. 80% of the PCE of the solar cells with ITO was achieved with bilayer polymer anode under illumination of  $100 \text{ mW cm}^{-2}$  due to complementary properties of two PEDOT forms in topography and conductivity, which indicates the potential to produce efficient flexible large-area polymer solar cells by roll to roll process at low temperatures.

We thank Professor Mats R. Andersson at Chalmers University of Technology for polymer supply. This work was financed by the Center of Organic Electronics at Linköping University, funded by the Strategic Research Foundation SSF. Yinhua Zhou acknowledges the scholarship from Chinese Scholarship Council (No. 2007U15021).

- <sup>1</sup>J. Peet, J. Y. Kim, N. E. Coates, W. L. Ma, D. Moses, A. J. Heeger, and G. C. Bazan, *Nat. Mater.* **6**, 497 (2007).
- <sup>2</sup>E. G. Wang, L. Wang, L. F. Lan, C. Luo, W. L. Zhuang, J. B. Peng, and Y. Cao, *Appl. Phys. Lett.* **92**, 033307 (2008).
- <sup>3</sup>J. Y. Kim, K. Lee, N. E. Coates, D. Moses, T. Q. Nguyen, M. Dante, and A. J. Heeger, *Science* **317**, 222 (2007).
- <sup>4</sup>M. Al-Ibrahim, H. K. Roth, and S. Sensfuss, *Appl. Phys. Lett.* **85**, 1481 (2004).
- <sup>5</sup>F. L. Zhang, M. Johansson, M. R. Andersson, J. C. Hummelen, and O. Inganäs, *Adv. Mater. (Weinheim, Ger.)* **14**, 662 (2002).
- <sup>6</sup>S. Admassie, F. L. Zhang, A. G. Manoj, M. Svensson, M. R. Andersson, and O. Inganäs, *Sol. Energy Mater. Sol. Cells* **90**, 133 (2006).
- <sup>7</sup>J. Huang, X. Wang, Y. Kim, A. J. deMello, D. D. C. Bradley, and J. C. Demello, *Phys. Chem. Chem. Phys.* **8**, 3904 (2006).
- <sup>8</sup>K. Tvingstedt and O. Inganäs, *Adv. Mater. (Weinheim, Ger.)* **19**, 2893 (2007).
- <sup>9</sup>K. Fehse, K. Walzer, K. Leo, W. Lovenich, and A. Elschner, *Adv. Mater. (Weinheim, Ger.)* **19**, 441 (2007).
- <sup>10</sup>E. Ahlswede, W. Muhleisen, M. W. M. Wahi, J. Hanisch, and M. Powalla, *Appl. Phys. Lett.* **92**, 143307 (2008).
- <sup>11</sup>See EPAPS Document No. E-APPLAB-92-090824 for transmission of three anodes and the statistical graphs of photovoltaic data of 45 solar cells (three kinds). For more information on EPAPS, see <http://www.aip.org/pubservs/epaps.html>
- <sup>12</sup>O. Inganäs, M. Svensson, F. Zhang, A. Gadisa, N. K. Persson, X. Wang, and M. R. Andersson, *Appl. Phys. A: Mater. Sci. Process.* **79**, 31 (2004).
- <sup>13</sup>C. J. Brabec, A. Cravino, D. Meissner, N. S. Sariciftci, T. Fromherz, M. T. Rispen, L. Sanchez, and J. C. Hummelen, *Adv. Funct. Mater.* **11**, 374 (2001).
- <sup>14</sup>V. D. Mihailetschi, P. W. M. Blom, J. C. Hummelen, and M. T. Rispen, *J. Appl. Phys.* **94**, 6849 (2003).
- <sup>15</sup>F. L. Zhang, A. Gadisa, O. Inganäs, M. Svensson, and M. R. Andersson, *Appl. Phys. Lett.* **84**, 3906 (2004).